Experimental Investigations on Machining of Silica Tiles using Acoustic Emission Technique

Kuppan P*
School of Mechanical and Building Sciences, VIT University, Vellore, Tamil Nadu, India

Nadadur Veeraraghavan Srikanth
Tata Consultancy Services, Chennai, Tamil Nadu, India

Xavier Arockia Raj
School of Mechanical Engineering, VIT University, Vellore, Tamil Nadu, India
Corresponding author, email: pkuppan@vit.ac.in

Abstract
In this paper, experimental investigations on machining of silica-silica composite using PCD tip insert cutter and electrodeposited diamond mills are presented. Acoustic emission (AE) sensing was employed for on-line monitoring of machining process. The results show that the electro deposited diamond coated tools are the best suited tool for machining silica tiles. The surface texture produced by end mill with fine grit size (D301) shows fine orientation of fibers when compared to PCD tip inserts and end mill with coarse grit size under the same cutting conditions.

***Keywords**: Silica-Silica composite tile, Acoustic Emission Technique (AET), PCD insert, Surface finish*

1 Introduction

The space shuttles use silica-based ceramic tiles as heat shield material and are made of high-purity amorphous silica fibres derived from common sand. Because of their low density, high porosity, high brittleness and fragility, machining of these material places stringent demands on the performance of the cutting tools [1].

The highly porous structure provides light weight and low thermal conductivity. The combination of the two provides thermal-shock resistance and strain tolerance. The porous and abrasive nature of silica tile leads to increased cutting tool wear rates.

Cutting strategies are to be identified to avoid excessive machining-induced damage to the work piece, to achieve a good surface finish and to achieve minimum tool wear. Suitable cutting tools need to be identified that can withstand the abrasive nature of the silica tile during machining and to achieve minimum wear. Optimum process parameters have to be identified which give rise to the best machining operation addressing the above problems.

Acoustic emission is one of the techniques used by many researchers for the online monitoring of machining process. Acoustic Emission refers to the class of phenomenon where transient elastic waves are generated due to rapid release of energy from localized sources. This generation of AE is a mechanical phenomenon. Mechanical deformation and fracture are the primary sources of AE signals. The energy thus released travels as a spherical wave front and can be picked up from the surface of a material using highly sensitive transducers. The output of each transducer/sensor is amplified through a low-noise amplifier, filtered to remove any noise. AE technique differs from other NDT methods as it detects anomaly in real time during the machining operation [2].

Several papers were published relating to acoustic emission technique and papers relating with this process used in silicon carbide and other ceramic materials [3-7]. However no papers could be found relating with AE technique used for silica – silica ceramic composite tile machining.

2 Objectives

The objectives of the present work are:

i. To determine the best process parameters for the machining of silica tiles.
ii. To determine the best cutting tool material for the machining of silica tiles.
iii. To investigate surface and subsurface damage if found during machining operation.

3 Experimental Setup

Emphasis is given to gain a comprehensive understanding of the acoustic emission generated in the machining of ceramics. Experiments were conducted in VIT University, Vellore. The photograph of the setup is given in Figure 1 and the schematic for the experimental setup is given in Figure 2.

Figure 1: Photograph of the experimental setup

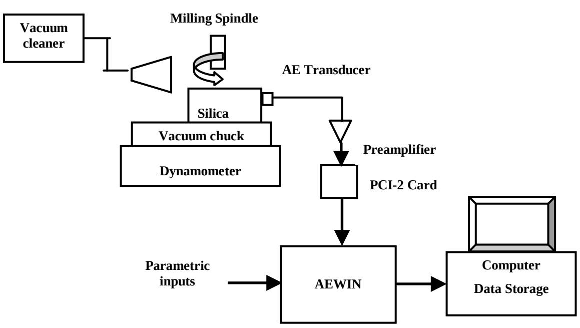

Figure 2: Schematic diagram of the experimental setup Photograph of the experimental setup

3.1 *Milling Machine Details*

The machining operations were performed in a 3-axes CNC vertical milling machine. It is a Kirloskar made vertical milling machine retrofitted with Siemens 802D controller. No cutting fluids were used during the machining process.

3.2 *Work piece Material*

Silica-silica ceramic tile (Figure 3(a) & 3(b)) used for spacecraft panels was chosen as work material. The properties of the work material are: (a) Flexural strength - 600-1000 kPa (b) Compressive strength - 400 - 800 kPa (c) Hardness - 80 Shore. The material is 90% porous in nature.

(a)

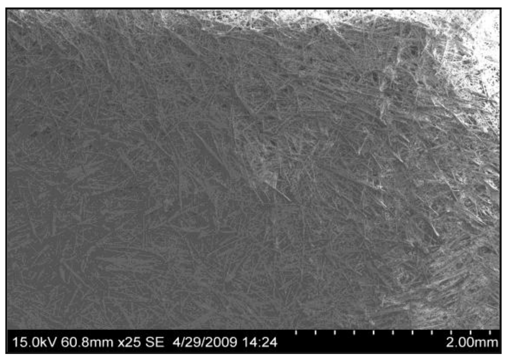

(b)

Figure 3: (a) Silica tile
(b) SEM image of Silica tile at 25x

3.3 *Tool Material*

From literature survey [8]–[11], it was found that the tools best suited for the machining of porous materials with minimum wear are PCD inserts and electrodeposited diamond end mill.

3.3.1 PCD inserts

(a) Insert shape – square
(b) Normal clearance angle – 15^o
(c) Size of insert – 9mm
(d) Thickness of insert – 3.97mm
(e) Nose rake angle – 45^o
(f) Cutting edge – rounded
(g) Direction of cut – right and left hand cutting
(h) PCD coating No – TN2510

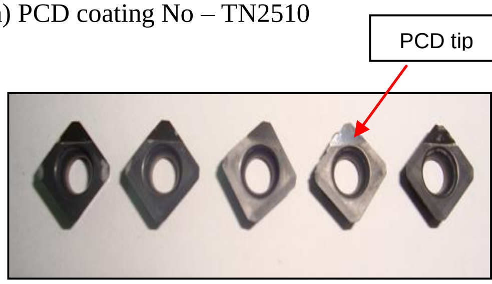

Figure 4: Photograph of the PCD inserts

3.3.2 Electrodeposited Diamond End mill

(a) Shank material : Steel
(b) Shank hardness : 60HRc
(c) Dynamic balancing : 2.5g at 15000 rpm

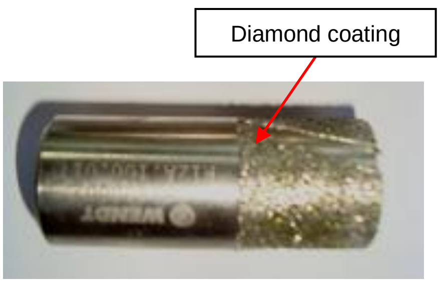

Figure 5: Photograph of the diamond end mill

3.4 *Work piece holding Device*

Due to the porous, abrasive and brittle nature of the silica tile common mechanical chucks cannot be used for holding the work piece. Hence a chuck is required that would not apply any compressive stress on the tile and would need only one surface of contact. A vacuum chuck is best suited for this operation. Hence a vacuum chuck is fabricated. The vacuum pressure to be used is 50 psi which is the standard vacuum pressure used in industries. The chuck needs to have enough strength to avoid buckling due to the vacuum pressure but at the same time should have enough cavity to create a good vacuum pressure. Bearing these factors in mind the vacuum chuck was designed with the suggested material of high carbon, high chromium steel with compressive strength and bending stress of 11000 kgf/cm^2 and 4000 kgf/cm^2 respectively.

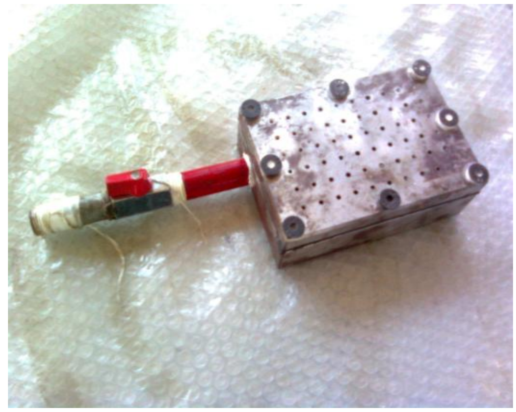

Figure 6: Photograph of Vacuum chuck

4 Design of Experiments

4.1 *Selection of Process Parameters*

Trial machining operations were performed prior to the actual machining operation on silica tile samples to select the process parameters and their ranges. The process parameters such as feed rate, cutting speed and depth of cut were varied at random to select the minimum and maximum range for the three parameters. The parameters and their levels are given in Table 1.

Table 1: The parameters and their values

Parameter	Unit	Level values		
		1	2	3
Cutting Speed	m/min	150	200	250
Feed Rate	mm/min	400	800	1200
Depth of Cut	mm	1	2	3

4.2 *Taguchi Design*

In the present study experiments are planned using Taguchi's experimental design. Taguchi method is one of the most important statistical tools for designing high quality systems at the reduced cost. This method uses a special design of orthogonal array to study the entire process parameter space with a smaller number of experiments. For the three process parameters L9 orthogonal array has been selected. Table 2 shows the design of experiments.

Table 2: Design of Experiments (L9 array)

Expt. No.	Cutting Speed (Vc) (m/min)	Feed Rate (f) (mm/min)	Depth of cut (d) (mm)
1	150	400	1
2	150	800	2
3	150	1200	3
4	200	400	2
5	200	800	3
6	200	1200	1
7	250	400	3
8	250	800	1
9	250	1200	2

5 Results and Discussion

5.1 *Machining of Silica tile using Polycrystalline Diamond tip cutter (PCD)*

Table 3 shows the surface roughness (Rt) value, maximum energy, RMS and amplitude values obtained after performing the nine experiments.

5.1.1 Discussion (PCD machining)

a) The maximum energy value increases as cutting speed, feed rate is increased (Figure 7). For depth of cut the energy value increases from minimum at 1mm depth of cut to maximum at 2mm depth of cut and reduces again as depth of cut is increased.

b) The maximum RMS value increases as cutting speed, feed rate is increased. For depth of cut the RMS value increases from minimum at 1mm depth of cut to maximum at 2mm depth of cut and reduces again as depth of cut is increased.

c) The maximum amplitude value increases as cutting speed, feed rate is increased. For depth of cut the amplitude value increases from minimum at 1mm depth of cut to maximum at 2mm depth of cut and reduces again as depth of cut is increased.

d) The surface roughness value reduces as cutting speed and feed rate is increased (Figure 8). For depth of cut the surface roughness value increases from minimum at 1mm depth of cut to maximum at 2mm depth of cut and reduces again as depth of cut is increased. Comparing this with acoustic emission values we can say that to have less surface roughness value high cutting speed and feed rate would be required.

Table 3: Maximum energy, RMS, Amplitude and R_t values for the various experiments

Expt. No.	Cutting speed (V_c) (m/min)	Feed rate (f) (mm/min)	Depth of cut (d) (mm)	Maximum Energy (Counts)	Maximum RMS (Volts)	Maximum Amplitude (dB)	Average Rt (μm)
1	150	400	1	2456	0.0386	73	102.00
2	150	800	2	15135	0.1162	79	105.53
3	150	1200	3	19636	0.1490	80	101.76
4	200	400	2	17227	0.1380	84	120.06
5	200	800	3	18113	0.1500	80	92.63
6	200	1200	1	3446	0.0918	76	93.96
7	250	400	3	11706	0.1794	84	109.01
8	250	800	1	21849	0.1744	83	94.75
9	250	1200	2	33345	0.2671	87	91.42

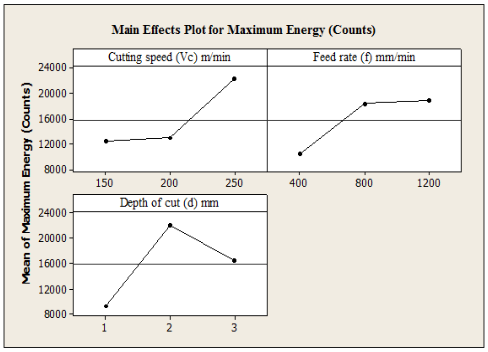

Figure 7: Maximum Energy plot of silica tile machining using PCD

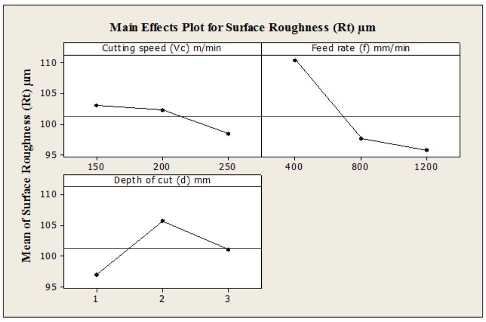

Figure 8: Surface roughness (R_t) plot of silica tile machining using PCD

From the point of view of acoustic emission we can safely correlate that high energy, RMS and amplitude value would be required to get a smooth surface finish [12] – [15]. This factor can be seen to be similar to the correlation formed by [16] in his paper 'real-time acoustic emission monitoring for surface damage in hard machining' where he found that in brittle material surface finish increases as RMS value is lowered similar to the one obtained in this experiment.

5.1.2 Waveform Analysis (PCD machining)

During the machining operation the waveform followed a specific pattern relating with the RMS value. It was found that RMS value increased until a particular value and began to fall during the first pass. This process was repeated when the tool took the second pass but the magnitude was found to diminish as it moved further away from the sensor. Hence it can be said that the magnitude of RMS value increases as it reaches closer to the proximity of the sensor. It was also found that the energy value also changes with a similar pattern. The amplitude however was found to be independent of the proximity range of the sensor and gave high amplitude values even when the tool was not in the close proximity of the acoustic emission sensor. The waveforms and the result during the experimentation are given in Figure 9(a) and 10(a) where Figure9 (a) represents the waveforms of sample 8 whereas Figure10 (a) represent the waveform of sample 9. As can be seen from the SEM photographs (Figure 9(b) and 10(b)) the fibers can be seen to be oriented uniformly in one direction for sample 8 whereas for sample 9 some disorientation can be observed. This can be attributed to the fact that depth of cut was 1mm for sample 8 and 2mm for sample 9 which caused the surface roughness to increase. This also correlates with the graph for surface roughness as shown in Figure 8. From the SEM photographs it can be seen that there is no surface damage or cracks mentioned that surface damage resulted in a single burst emission or discontinuous acoustic emission from the work piece during machining operation. According [16] in case of no surface damage there won't be any discontinuous emission. As can be seen from the waveforms there is no discontinuous emission and hence it can be confirmed that surface damage does not occur in materials which give uniform acoustic emission during machining.

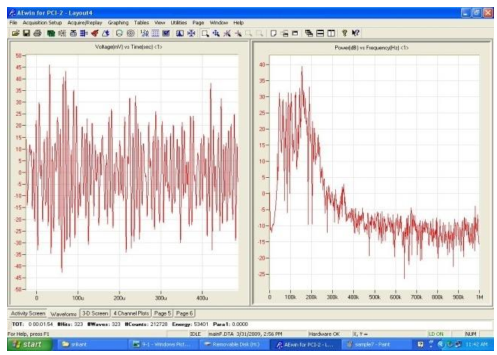

(a)

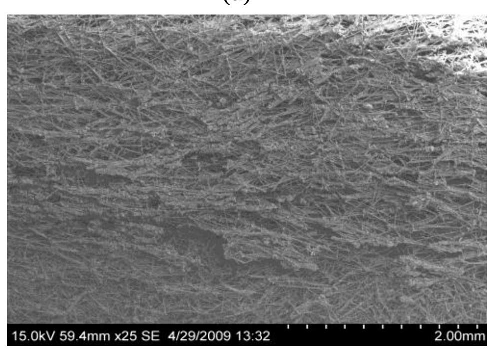

(b)

Figure 9: (a) Waveforms formed during machining of sample 8 and (b) SEM photograph of sample 8 at 25x magnification

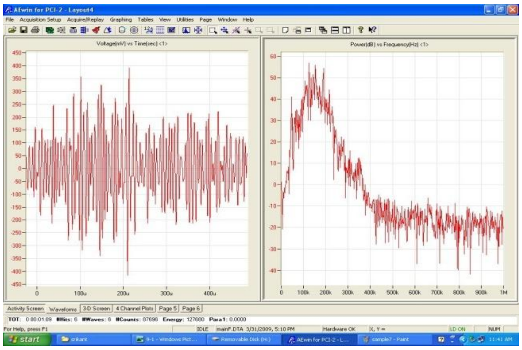

(a)

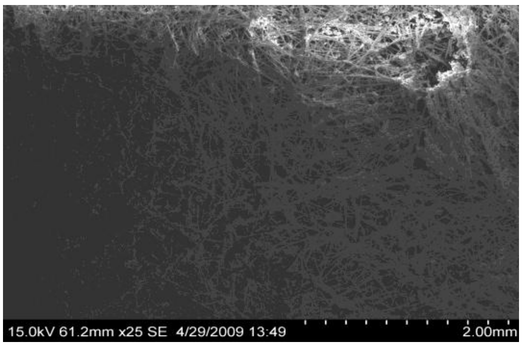

(b)

Figure 10: (a) Waveforms formed during machining of sample 9 and (b) SEM photograph of sample 9 at 25x magnification

5.2 *Machining of silica tile using Electrodeposited Diamond End Mill (coarse grain)*

5.2.1 Discussion (Electrodeposited Diamond End mill (coarse grain))

(a) The energy value increases as cutting speed is increased until the speed has reached a mid value after which it decreases at the same rate (Figure 11). The maximum energy value increases uniformly as feed rate is increased. For depth of cut the maximum energy decreases until it reaches a minimum value at mid level after which it increases again.

(b) The RMS value increases as cutting speed is increased until the speed has reached a mid value after which it decreases at the same rate. The maximum RMS value increases continuously as feed rate is increased. For depth of cut the maximum RMS decreases until it reaches a minimum value at mid level after which it increases again.

(c) The amplitude value varies linearly with the cutting speed. As cutting speed is increased the amplitude value decreases uniformly. For feed rate the maximum amplitude value increases until it reaches the mid value of feed rate after which the amplitude value reduces. The amplitude value increases linearly as depth of cut is increased in a uniform manner

(d) The surface roughness decrease as feed rate is increased and increases when depth of cut is increased (Figure 12). In the case of cutting speed surface roughness increases initially with increase in cutting speed until a maximum value is reached at 2mm depth of cut after which it begins to fall rapidly as it is increased further. This can be accounted for the fact that there are decreased amount of burst emission due to which cutting speed does not have any affect on the surface roughness.

Table 4: Maximum energy, RMS, Amplitude and Avg. R_t values for the various experiments

Expt. No.	Cutting speed (V_c) (m/min)	Feed rate (f)(mm/min)	Depth (d) (mm)	Max Energy (Counts)	Max RMS (Volts)	Max Amplitude (dB)	Avg Rt (µm)
1	150	400	1	368	0.0172	69	84.16
2	150	800	2	575	0.0204	82	86.68
3	150	1200	3	5393	0.0420	91	76.67
4	200	400	2	413	0.0214	76	95.34
5	200	800	3	8345	0.0652	90	93.73
6	200	1200	1	5144	0.0390	71	83.72
7	250	400	3	3377	0.0300	74	94.33
8	250	800	1	341	0.0218	78	72.83
9	250	1200	2	1501	0.0282	78	85.62

e) The surface roughness varies almost linearly with energy as maximum energy plot in case of cutting speed shows a minimum energy value at the same point as the maximum surface roughness and vice versa. Hence it can be said that higher energy value gives rise to a low surface roughness.

The same plots are obtained even in the case of maximum RMS and so the same correlation can be obtained. In the case of maximum amplitude plots cutting speed does not show much variation in the amplitude. The amplitude variation with feed rate is similar to the energy and RMS plots and so it can be said that large amplitude may have some effect in obtaining low surface roughness.

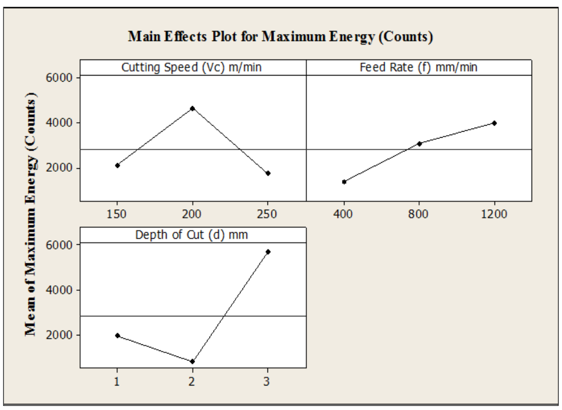

Figure 11: Max. Energy plot of silica tile machining using Electrodeposited Diamond End mill (coarse grain)

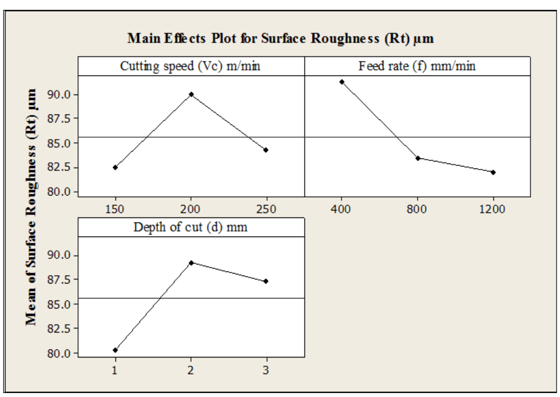

Figure 12: Surface roughness plot of silica tile machining using Electrodeposited Diamond End mill (coarse grain)

5.2.2 Waveform Analysis (Electrodeposited Diamond End mill (coarse grain))

The waveforms were found to follow a similar pattern to that was obtained during PCD machining. However in this case the magnitude and RMS obtained was found to be much less than that found during PCD machining. The waveforms and the result during the experimentation are given in Figure 13 (a) and 14 (a) where Figure 13 (a) represents the waveforms of sample 3 whereas Figure 14(a) represent the waveform of sample 5. As can be seen from the SEM photographs (Figure 13(b) and 14(b)) the fibers can be seen to be oriented disproportionately for both the samples.

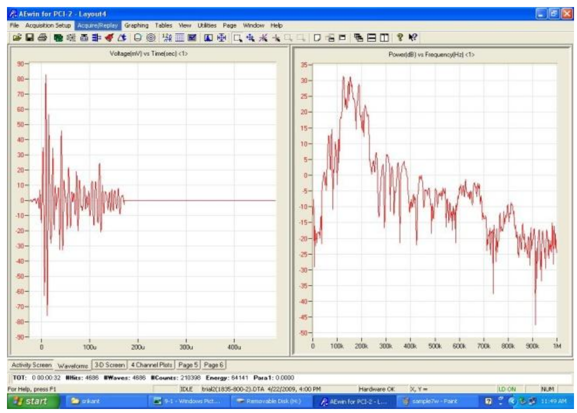

(a)

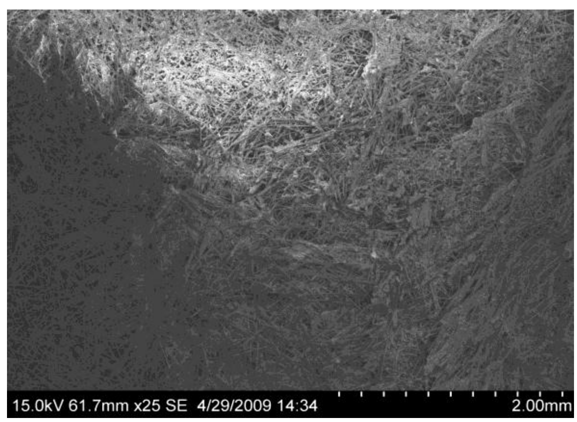

(b)

Figure 13: (a) waveforms formed during machining of sample 3 (b) Microstructure view of sample 3 using SEM at 25x magnification

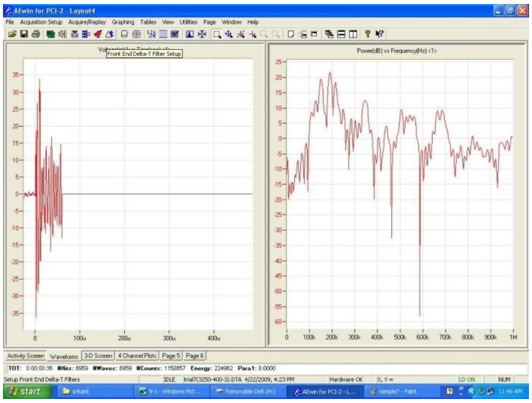

(a)

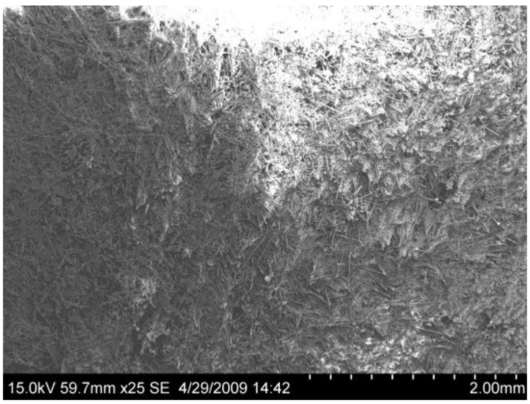

(b)

Figure 14: (a) waveforms formed during machining of sample 5 (b) Microstructure view of sample 5 using SEM at 25x magnification

This is because of the use of coarse electrodeposited diamond end mill as the samples viewed in this case have lower process parameters than those viewed in the case of PCD machining

5.3 *Machining of silica tile using Electrodeposited Diamond End Mill (fine grain)*

5.3.1 Discussion (Electrodeposited Diamond End mill (fine grain))

a) The maximum energy value decreases as cutting speed is increased to a minimum value at the mid point after which there is an increase again as cutting speed is increased (Figure 15). It follows the same pattern in case of feed rate. In the case of depth of cut the energy value increases until the mid value of depth of cut is reached after which it again starts to reduce

b) The maximum RMS value decreases as cutting speed is increased to a minimum value at the mid point after which there is an increase again as cutting speed is increased. It follows the same pattern in case of feed rate. In the case of depth of cut the RMS value increases until the mid value of depth of cut is reached after which it again starts to reduce

c) In the case of maximum amplitude variation it increases very slightly as cutting speed is increased. The increase is more as feed rate is increased and becomes steeper in the case of depth of cut.

Table 5: Maximum energy, RMS, Amplitude and Avg. R_t values for the various

Expt. No.	Cutting speed (V_c) (m/min)	Feed rate (f)(mm/min)	Depth (d) (mm)	Max Energy (Counts)	Max RMS (Volts)	Max Amplitude (dB)	Avg Rt (µm)
1	150	400	1	11181	0.0980	78	84.16
2	150	800	2	6657	0.0528	73	86.68
3	150	1200	3	17545	0.1376	86	76.67
4	200	400	2	14906	0.1250	79	95.34
5	200	800	3	11373	0.0928	86	93.73
6	200	1200	1	6929	0.0562	73	83.72
7	250	400	3	8806	0.0768	75	103.23
8	250	800	1	13192	0.1186	80	89.38
9	250	1200	2	23363	0.1890	83	85.62

d) The surface roughness shows a linear relation with cutting speed and feed rate. Increase in cutting speed causes a decrease in surface roughness whereas increase in feed rate causes an increase in surface roughness (Figure 16). Depth of cut shows erratic variations with surface roughness increasing rapidly until 2mm depth of cut is reached and then showing a rapid decrease as depth of cut is increased.

e) Since both maximum energy and RMS plots show a linear increase in their value as cutting speed and feed rate is increased, these signals cannot be used to determine the surface finish of the silica tile. This is because increase in cutting speed causes a decrease in surface roughness whereas increase in feed rate causes an increase in surface roughness. However in the case of maximum Amplitude plots it can be seen that amplitude does not vary when cutting speed is increased whereas it increases rapidly as feed rate is increases. Hence it can be said that higher amplitude leads to a low surface roughness going by the amplitude and surface roughness plot of feed rate.

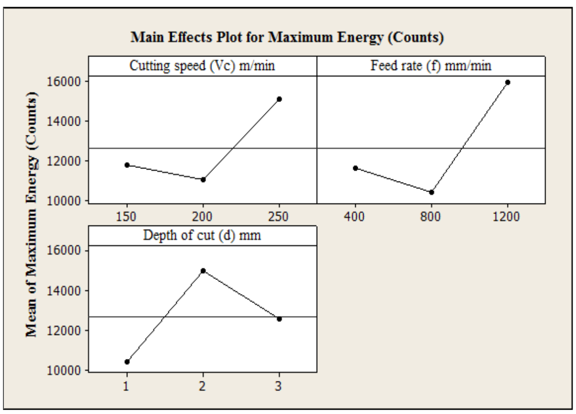

Figure 15: Max. Energy plot of silica tile machining using Electrodeposited Diamond End mill (fine grain)

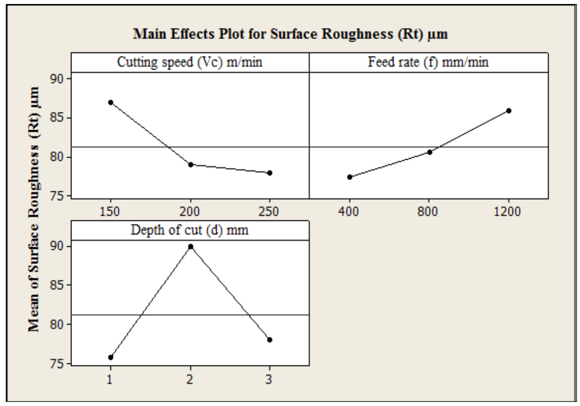

Figure 16: Surface roughness plot of silica tile machining using Electrodeposited Diamond End mill (fine grain)

5.3.2 Waveform Analysis (Electrodeposited Diamond End mill (fine grain))

The waveforms were found to follow a similar pattern to that was obtained during PCD machining. The waveforms and the result during the experimentation are given in Figure 17(a) and 18(a) where Figure 17(a) represents the waveforms of sample 3 whereas Figure 18(a) represent the waveform of sample 9. As can be seen from the SEM photographs (Figure 17(b) and 18(b)) the fibres can be seen to be oriented uniformly in one direction for both sample 3 and 9. Due to the use of fine electrodeposited diamond end mill all the samples have been found to have a smooth finish unlike the case of PCD machining and coarse end mill. However for finer finish using this tool it can be seen that high cutting speed and low feed rate would be required in this case to get the best surface finish.

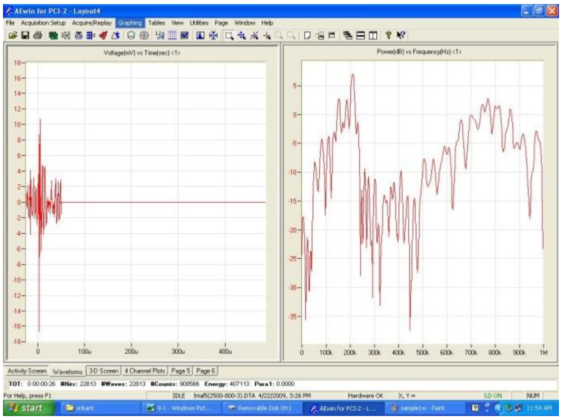

(a)

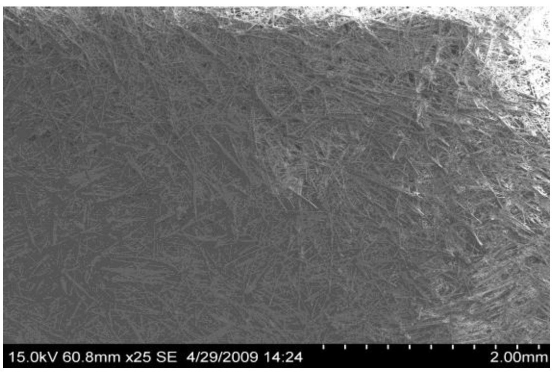

(b)

Figure 17: (a) waveforms formed during machining of sample 3 (b) Microstructure view of sample 3 using SEM at 25x magnification

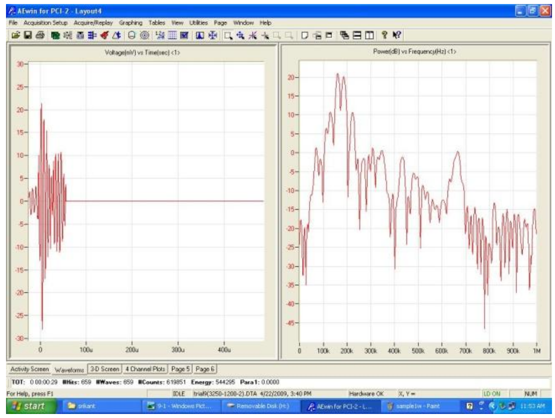

(a)

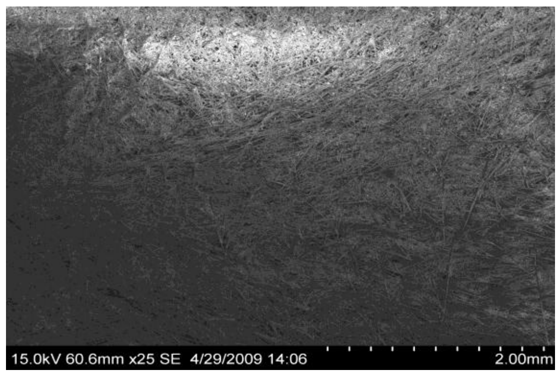

(b)

Figure 18: (a) waveforms formed during machining of sample 9 (b) Microstructure view of sample 9 using SEM at 25x magnification

6 Conclusions

From the machining experiments and the analysis of AE signals the following main conclusions are drawn:

a) High cutting speed and feed rate resulted in low values of surface roughness during machining with PCD tip insert.

b) From the acoustic emission signals the surface roughness is found less in those samples which gave high energy, RMS and amplitude during machining with PCD insert.

c) Machining with coarse electrodeposited diamond end mill produces the least surface roughness at high feed rate.

d) The surface roughness is found less in those samples which gave high amplitude in coarse electrodeposited diamond end mill machining. Also high energy and RMS value above 250 m/min cutting speed resulted in low surface roughness.

e) From the acoustic emission signals the surface roughness is found less in those samples which gave high amplitude in fine electrodeposited diamond end mill machining and was found to be independent of high energy and RMS value.

f) The electro deposited diamond coated end mill with grit D301 produces good surface finish.

Acknowledgments

The authors would like to thank the Aeronautical Research and Development Board, Government of India for the financial support and Vikram Sarabhai Space Center, Trivandrum for providing the Silica tile samples.

References

[1] Norms Revenge, "The Space Shuttle Orbiter and Ceramic Tiles – Some History and Information", LMCO/NASA KSC, 2003

[2] Charles J. Hellier, "*Handbook of Non destructive Evaluation*", MGH 2001

[3] Tuersley, I.P., Jawaid, A., and Pashby, I.R., "*Various methods of machining advanced ceramic materials*", Journal of Materials Processing Technology ,(1994) pp 377-390

[4] S. Arul, L. Vijayaraghavan, S.K. Malhotra, "*Online monitoring of acoustic emission for qualitycontrol in drilling of polymeric composites*", Journal of Materials Processing Technology(2007), pp 184-190

[5] Qingliang Zhaoa, Yingchun Lianga, David Stephensonb, John Corbett, "*Surface and subsurface integrity in diamond grinding of optical glasses on Tetraform 'C'* ", International Journal of Machine Tools & Manufacture (2007), pp.2091–2097

[6] W. Yao, Z. Li and M. Qi, *Damage Process Detection of a Ceramic Tile System by Acoustic Emission*, Experimental Mechanics, Vol. 40, No. 3, 2000, pp.265-270

[7] Kun Li and T. Warren Liao, "*Surface/subsurface damage and the fracture strength of ground ceramics*", Journal of Materials Processing Technology (1996), pp 207-220

[8] Dolinsek, S., and Kopac, J., *Acoustic emission signals for tool wear identification*, Wear 1999. pp 295–303

[9] Bao.W.Y., Tansel.I.N.,*Modeling micro-end-milling operations. Part III: influence of tool wear*, International Journal of Machine Tools & Manufacture 40 (2000) pp 2193

[10] Abdul B. S. and Raman.S. (1987). *Detection of tool flank wear using acoustic signature analysis*, Wear, Vol. 115(3), pp. 265-272.

[11] Aue, J., and De Hosson, J.Th M., *A study of the mechanical properties of highly porous ceramics using acoustic emission*, Journal of Materials Science 33 (1998) pp 5455 – 5462

[12] Marinescu, I., and Axinte, A.D., *A critical analysis of effectiveness of acoustic emission signals to detect tool and workpiece malfunctions in milling operations*, International Journal of Machine Tools & Manufacture 48 (2008), pp 1148–1160

[13] Byrne, G. and Barry, J., "*Chip Formation, Acoustic Emission and Surface White Layers in Hard Machining*", CIRP Annals, Vol. 51(1), pp. 65-70.

[14] Beggan, C., Woulfe, M., Young, P. and Byrne, G. (1999)." *Using Acoustic Emission to Predict Surface Quality*", Int. J. Adv. Manuf. Technol., Vol. 15, pp. 737-742.

[15] Dunegan, H. L., "*A new acoustic emission technique for detecting and locating growing cracks in complex structures*", May 2000 to be published

[16] Guo, Y.B., and Ammula, S.C., "*Real-time acoustic emission monitoring for surface damage in hard machining*", International Journal of Machine Tools & Manufacture 45 (2005), pp 1622–1627